Journal of Physics:
Conference Series

PAPER • **OPEN ACCESS**

Challenges in simulating the wind over a coastal complex-shaped site: Madeira Island

To cite this article: I L Coimbra and J M L M Palma 2024 *J. Phys.: Conf. Ser.* **2767** 052014

Journal of Physics: Conference Series **2767** (2024) 052014 doi:10.1088/1742-6596/2767/5/052014

Challenges in simulating the wind over a coastal complex-shaped site: Madeira Island

I L Coimbra and J M L M Palma

University of Porto (UPORTO), Faculdade de Engenharia da Universidade do Porto, Rua Dr Roberto Frias s/n, 4200-465 Porto, Portugal

E-mail: `isadora.coimbra@fe.up.pt`

Abstract. The wind behaviour on Madeira Island is shaped by the intricate coastline and mountainous terrain, features that are not easily represented in numerical models. Thus, this study addressed some challenges and possible solutions in setting up a meso-to-microscale model chain, with the WRF (1-km mesh) and VENTOS®/M (50-m mesh in the high-resolution area) models, in Madeira's coastal and complex terrain. Wind measurements from four meteorological towers (located in the eastern peninsula–T0978/E–and on the SE–T0521/SE, S–T0522/S, and N–T0960/N–coasts) served as references to assess the simulations. First, due to WRF's `landmask` position, land areas were misclassified as sea (and vice versa). This issue was addressed by altering the domain position to better allocate the `landmask` on the east peninsula, resulting in improved near-surface wind simulations at T0978/E (reducing RMSE and bias by 19% and 67%). Secondly, WRF's default interpolation of the `SST` variable did not account for missing and masked data. As such, a different `SST` interpolation method was employed, leading to improved near-surface wind simulations at T0960/N (reducing RMSE and bias by 11% and 84%) and T0522/S (10% and 16% reduction) masts, but higher errors at T0978/E (7% and 45% increase). The negative influence arose from an incorrect speedup with the new interpolation method. Thirdly, the impact of `SST_SKIN`, which influences the temperature distribution at the skin level, was evaluated in WRF. Activating `SST_SKIN` led to a slight improvement in the near-surface wind simulation only at T0521/SE (2% and 6% RMSE and bias reduction), probably due to the dominant smaller-scale nature of the atmospheric circulation in the area, which contrasts with the circulation at the other towers, dominated by the trade winds (N and E masts) and the Island's wake (S mast). When using the WRF outputs as boundary conditions, these effects on the microscale runs were less pronounced than on the mesoscale results. Nonetheless, the RMSE and bias of the near-surface wind simulation in VENTOS®/M were reduced by 6% and 9% at T0978/E.

1. Introduction

Located in the North Atlantic Ocean, with an area of 741 km^2 and 150 km of coastline, Madeira Island, part of the eponymous archipelago, has complex terrain of volcanic origin with an NW-SE mountain range, 50 km long and 25 km wide [1], Fig. 1. The weather in Madeira is greatly influenced by the Azores high [2] and the northeasterly trade winds [3] on the synoptic scale, while, in the meso- and microscale, the land-sea transition and complex terrain modify the atmospheric circulations. On the Island's leeward (SW) side, a wake is formed, with warm and dry eddies and high lateral horizontal wind shear [1], and two tip jets develop on the Island's flanks [4]. The turbulence arising from the wake and the tip jets, among other atmospheric

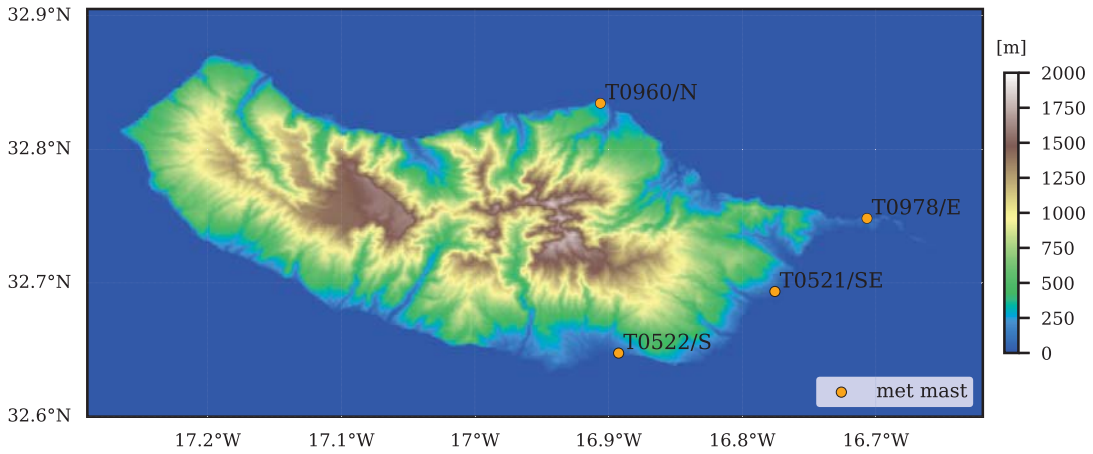

Figure 1. Madeira Island terrain [7] and meteorological tower locations.

phenomena related to the complex terrain and the coastal region, affect the Southern part of Madeira Island and its airport activities [4, 2].

Several studies highlighted the complex wind-terrain interaction in Madeira [3, 1, 2, 4]. However, these studies lack multiple wind measurements and high-resolution wind simulations. Therefore, we started to analyse the wind behaviour on the Island by employing met-mast measurements and high-resolution atmospheric simulations with a one-way meso-to-microscale coupling, composed of the Weather Research and Forecasting (WRF) model [5] and the VENTOS®/M model [6]. During this process, we encountered some challenges in setting up the simulation models, particularly WRF, in this coastal and complex-shaped site.

Due to the difficulties encountered in simulating the wind over Madeira and the tendency of most simulation studies to focus on results without addressing practical problems in setting up atmospheric simulations, this work aims to highlight some of these problems, suggest solutions, and analyse their impact on the simulation results. For this purpose, we investigated simulations employing the widely-used WRF mesoscale model and the VENTOS®/M URANS microscale model, using measurements from four meteorological stations across the island as references.

2. Methodology

The study covered a period in 2016 (7 Aug 00:00 – 8 Aug 12:00) when extreme wind conditions adversely affected the Island [2].

2.1. Measurements

Ten-minute wind measurements from cup anemometers at four meteorological stations (Fig. 1)—T0960/N, T0978/E, and T0522/S at 10 m a.g.l. and T0521/SE at 14 m a.g.l.—were used to assess the accuracy of the simulation results, based on Root Mean Square Error (RMSE) and systematic error (bias).

2.2. Simulations

The simulations employed first the WRF model (version 4.2.1) and later the VENTOS®/M model, in an offline one-way meso-to-microscale model chain. The mesoscale model was configured with three one-way nested domains of 9-, 3-, and 1-km horizontal grid spacing, covering the entire Island. In contrast, the microscale model had a 50-m horizontal mesh in

the high-resolution area (25 km^2 in the SE of the Island) that expanded up to the resolution of WRF's finest mesh, approximately, covering the eastern half of the island.

The ERA5 dataset [8] was used as input to the WRF model, containing the Sea Surface Temperature (`SST`) and Sea Surface Skin Temperature (`SST_SKIN`) variables due to the coastal characteristic of the site. Since the topography in Madeira plays an important role in the wind behaviour, the runs employed a topography map of Madeira Island with 5-m horizontal resolution, resampled to the horizontal mesh of each run. The Global Multi-resolution Terrain Elevation Data (GMTED2010) [9] described the terrain of the other Islands in the archipelago. Land use maps were imported from CORINE Land Cover 2012 [10], with 100-m resolution, adapted for WRF [11], and employed together with the New European Wind Atlas lookup table [12].

The main WRF parameterisations were: WRF Single–Moment 6–Class [13] microphysics scheme, Rapid Radiative Transfer Model [14] and Dudhia [15] for the long-wave and short-wave radiation, revised MM5 [16] scheme for the surface-layer, Unified Noah [17] land surface scheme, Yonsei University [18] for the planetary boundary layer, and Grell-Freitas [19] for cumulus.

The coupling between WRF and VENTOS®/M [6] is one-way and offline, made by prescribing interpolated WRF results at the microscale domain's boundaries. At the lateral boundaries, the mean velocity components and dry potential temperature (three-dimensional fields) are linearly interpolated from the WRF mesh into the VENTOS®/M grid every 5 minutes, while the boundary-layer height (a two-dimensional field) is interpolated only at the first timestamp to generate initial profiles of k and ε. At the domain bottom, the microscale domain receives from WRF the linearly interpolated surface heat flux (`HFX`) and surface skin temperature (`TSK`) every 5 minutes. Neumann conditions are used for the turbulence variables (k, ε).

Since VENTOS®/M uses a non-uniform mesh, only T0521/SE (our primary region of interest) was situated in the 50-m mesh area. At other tower locations, the grid sizes were larger: 628 m × 798 m at T0960/N, 442 m × 165 m at T0978/E, and 546 m × 450 m at T0522/S.

3. Results and discussion

When setting up the mesoscale simulations for Madeira, we noticed that the positioning of the `landmask` variable, the `SST` interpolation method, and the `SST_SKIN` update impacted the WRF results. Consequently, these changes in WRF parameters also influenced the microscale simulations, since variables from WRF were used as input in the VENTOS®/M model.

Therefore, the following results address WRF `landmask`, `SST`, and `SST_SKIN` parameters and their influences on mesoscale runs. The cumulative effect of these changes in the model chain is then evaluated in two VENTOS®/M simulations: one using WRF results with default settings and another with modified settings.

3.1. The influence of the `landmask` *variable positioning on the mesoscale run*

Madeira's complex-shaped coastline cannot be accurately described by a 1-km horizontal mesh. However, depending on the positioning of the mesoscale domain, important features for the flow on the Island may or may not be included in the domain representation. For example, when we first positioned the WRF domain (domain position 1—DP1), the Madeira E peninsula (called Ponta de São Lourenço), which houses an operational wind farm, was wrongly classified as a sea area (Fig. 2a, red circle). This occurred because the grid cells encompassing this peninsula had more than 50% of their area assigned as water bodies, a variable that comes from the land-use dataset (CORINE Land Cover), leading WRF to classify this area as water in its `landmask` variable. The land-sea misclassification directly influences all the variables that depend on the land categorisation in WRF, such as surface properties, surface fluxes, and boundary layer parameterisation, while indirectly affecting the wind behaviour.

To allocate the `landmask` better at Madeira E peninsula, we shifted the WRF domain position northwards (domain position 2—DP2), ensuring that the finer mesh cells covered the majority

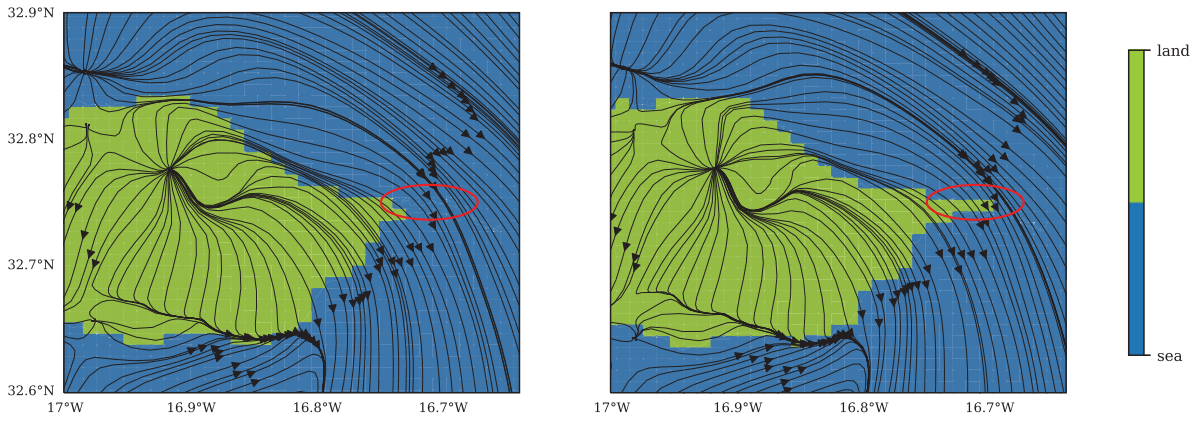

Figure 2. Streamlines of WRF instantaneous wind at 10 m a.g.l. (8 Aug 2016, 00:00) above the `landmask` for two domain placements: DP1 (a) and DP2 (b). The white line represents Madeira's true coastline, and the plot grid lines (light grey) match the 1-km WRF grid cells.

Table 1. Statistical metrics of the simulated near-surface wind.

Tower	Metric	WRF				VENTOS®/M	
	$[\mathrm{m\,s^{-1}}]$	DP1	DP2	DP2-MM	DP2-MM-S	DP1	DP2-MM-S
T0960/N	RMSE	1.17	1.27	1.13	1.17	1.20	1.34
	bias	0.35	0.43	0.07	0.04	0.58	0.48
T0978/E	RMSE	2.20	1.79	1.92	1.96	2.18	2.05
	bias	1.35	0.44	0.64	0.70	1.35	1.23
T0521/SE	RMSE	3.26	3.32	3.35	3.28	3.36	3.36
	bias	−0.74	-0.90	−1.03	−0.97	0.33	0.34
T0522/S	RMSE	2.18	2.20	1.99	2.02	3.44	3.47
	bias	1.49	1.52	1.28	1.36	2.88	2.90

of the peninsula's terrain (Fig. 2b, red circle). The influence of the `landmask` placement, due solely to the domain positioning, on the simulated near-surface wind (10 m a.g.l.) is presented in Fig. 2 (see Fig. A1 for mean horizontal wind speed differences).

By modifying the `landmask` position through the WRF domain location, the RMSE and bias of the simulated wind speed were reduced by 19% (from $2.20\,\mathrm{m\,s^{-1}}$ to $1.79\,\mathrm{m\,s^{-1}}$) and 67% (from $1.35\,\mathrm{m\,s^{-1}}$ to $0.44\,\mathrm{m\,s^{-1}}$) at T0978/E (Table 1), located in Ponta de São Lourenço. Compared to WRF-DP1 results, WRF-DP2 showed a consistent offset in wind speed (around $1\,\mathrm{m\,s^{-1}}$ lower) throughout the entire period, attributed to the higher surface roughness at T0978/E with the improved `landmask` position. At other tower sites, the average wind speed showed similar values in both WRF runs (Table 1), as the `landmask` classification was not altered in these grid cells.

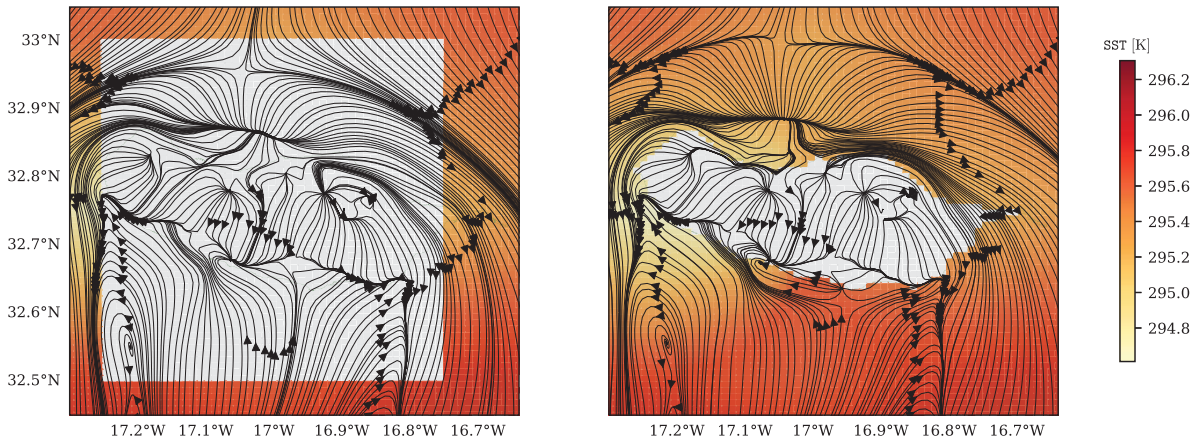

Figure 3. Streamlines of WRF instantaneous wind at 10 m a.g.l. (7 Aug 2016, 22:00) above the `SST` for two `SST` interpolation methods: default (a) and modified (b).

3.2. The influence of the `SST` *variable interpolation on the mesoscale run*

Besides the land-use data, WRF also requires a global atmospheric dataset, such as ERA5, to provide boundary conditions for the runs. In this process, ERA5 variables, originally from a ∼30-km mesh, are interpolated into the mesoscale domain according to the parameters in the `METGRID.TBL` table. However, when we used the WRF default interpolation of the `SST` variable (`sixteen_pt+four_pt`), many grid cells near the Madeira coastline were not assigned with `SST` values, as indicated by the white region in Fig. 3a. This lack of `SST` data, which can adversely impact the model's results, occurred because the default interpolation method could not handle missing or masked data, and the ERA5 `SST` is a masked variable with a coarse mesh.

To correct the gaps in the WRF's `SST`, we modified the `METGRID.TBL` file. The `SST` interpolation option was updated to consider missing and masked data, by adding the weighted-average interpolation method, and a mask (from `landmask`) was assigned to prevent data points from being interpolated over land cells. These changes modified the sea surface temperature distribution, Fig. 3b (at the sea white region in Fig. 3a), and impacted the near-surface wind in the mesoscale run (see Fig. A2 for mean horizontal wind speed differences), mainly at T0960/N and T0522/S, located on Madeira's North and South coastline (Fig. 1).

Compared to the original `METGRID.TBL` (WRF DP2), the modified `METGRID.TBL` (WRF DP2-MM) reduced the RMSE and bias of the near-surface wind by 11% and 84% at T0960/N (from $1.27\,\mathrm{m\,s^{-1}}$ and $0.43\,\mathrm{m\,s^{-1}}$ to $1.13\,\mathrm{m\,s^{-1}}$ and $0.07\,\mathrm{m\,s^{-1}}$), and 10% and 16% at T0522/S (from $2.20\,\mathrm{m\,s^{-1}}$ and $1.52\,\mathrm{m\,s^{-1}}$ to $1.99\,\mathrm{m\,s^{-1}}$ and $1.28\,\mathrm{m\,s^{-1}}$), Table 1. Conversely, at T0978/E, the RMSE and bias increased by 7% and 45% (from $1.79\,\mathrm{m\,s^{-1}}$ and $0.44\,\mathrm{m\,s^{-1}}$ to $1.92\,\mathrm{m\,s^{-1}}$ and $0.64\,\mathrm{m\,s^{-1}}$), due to the incorrect wind acceleration in the WRF DP2 simulation from 21:00 to 3:00, between the 7th and 8th of August. At T0521/SE, the near-surface wind was less affected by the `SST` modification in `METGRID.TBL`, resulting in similar errors between WRF DP2-MM and WRF DP2.

3.3. The influence of activating `SST_SKIN` *on the mesoscale run*

A third configuration test involved activating the sea surface skin temperature [20] within the WRF run (on the `namelist.input` file). The `SST_SKIN` also comes from the ERA5 input dataset and represents the immediate sea surface temperature (at skin level), directly influenced by solar

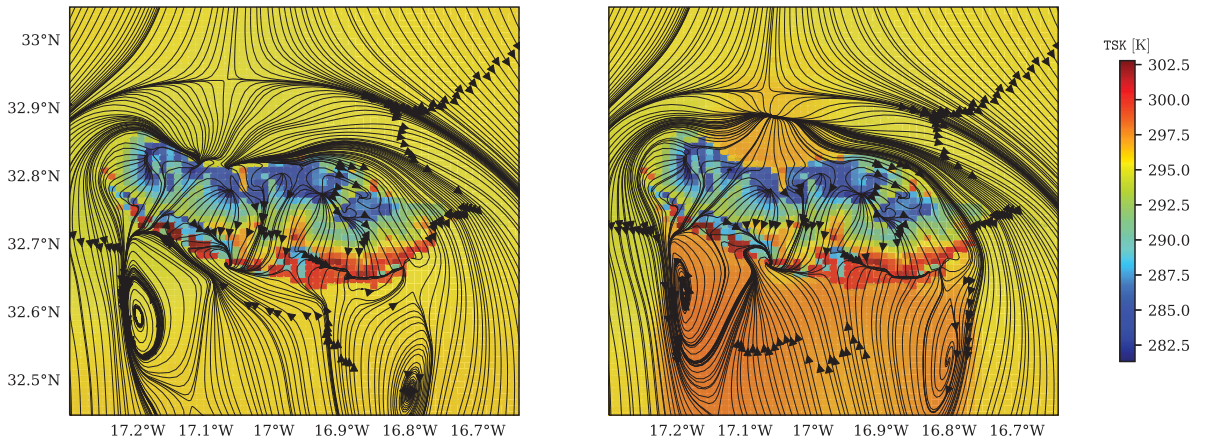

(a) (b)

Figure 4. Streamlines of WRF instantaneous simulated wind at 10 m a.g.l. (7 Aug 2016, 20:00) above the surface skin temperature (`TSK`) for two mesoscale runs: without (a) and with `SST_SKIN` update (b).

heating. This differs from the `SST` variable, which accounts for the temperature below the sea surface level and presents higher thermal inertia. Nonetheless, both input parameters play an important role in representing atmosphere-ocean interactions.

In a default WRF run, `SST_SKIN` is not activated, and the model uses the `SST` as the skin temperature at sea level (Fig. 4a). However, activating `SST_SKIN` in the mesoscale run directly impacted the surface skin temperature (Fig. 4b) and led to subtle changes in Madeira's wind simulations (see Fig. A3 for mean horizontal wind speed differences), namely at T0521/SE, T0978/E, and T0960/N.

Between the configurations analysed, the `SST_SKIN` had the least impact on the simulated near-surface wind (Table 1). At T0521/SE, the wind simulation improved with `SST_SKIN`, reducing the RMSE and bias by 2% (from $3.35\,\mathrm{m\,s^{-1}}$ to $3.28\,\mathrm{m\,s^{-1}}$) and 6% (from $-1.03\,\mathrm{m\,s^{-1}}$ to $-0.97\,\mathrm{m\,s^{-1}}$). On the other hand, the `SST_SKIN` had a negative impact on the simulated wind at T0960/N, T0978/E, and T0522/S, increasing 4%, 2%, and 1% the RMSE, respectively. This is attributed to the different atmospheric conditions at each tower location, where T0960/N and T0978/E are primarily affected by the trade winds and T0522/S by the Island's wake, whereas T0521/SE seems to be more influenced by smaller-scale phenomena and, therefore, more sensitive to `SST_SKIN`.

3.4. The influence on the microscale run

Lastly, the effects of the WRF changes were assessed when employing mesoscale results as boundary conditions to microscale runs. Direct comparisons between WRF and VENTOS®/M results are not recommended due to intrinsic data differences. Despite both sets of results being reduced to 10-minute averages, VENTOS®/M wind-speed time series tended to show more oscillation due to its smaller mesh, lower time step, and more detailed terrain, in contrast to WRF's smoother time series. This difference is reflected in the RMSE and bias values (Table 1), as these metrics generally favour smoother data series [21]. As such, the comparisons here focused on the different runs performed for each model.

To quantify how the `landmask` classification, `SST` interpolation, and `SST_SKIN` activation in WRF affected the microscale results, two VENTOS®/M simulations were carried out: DP1

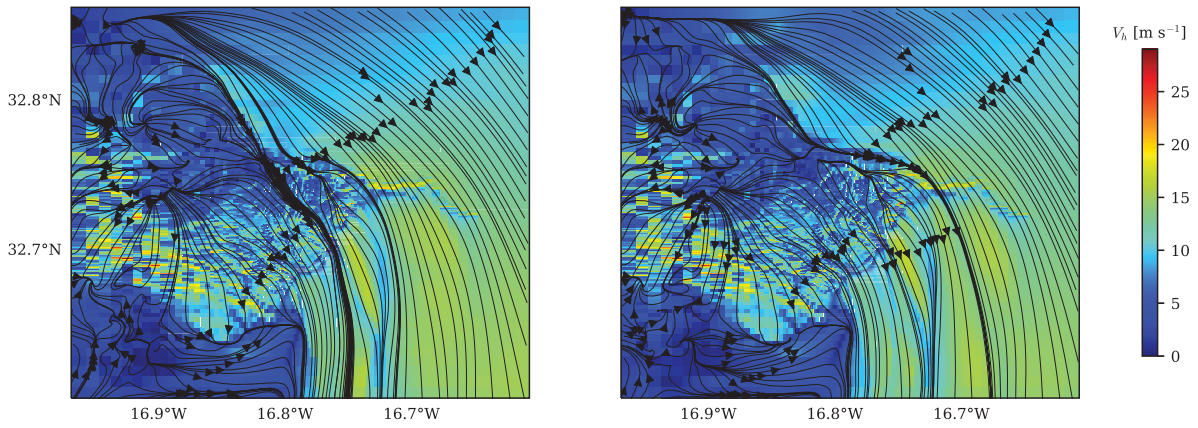

Figure 5. Streamlines of VENTOS®/M instantaneous wind at 10 m a.g.l. (07 Aug 2016, 23:00) above the horizontal wind speed (V_h) for two microscale runs: DP1 (a) and DP2-MM-S (b).

(Fig. 5a) and DP2-MM-S (Fig. 5b). The first used mesoscale results obtained with the WRF's default parameters (original `SST` interpolation, no `SST_SKIN` activation) and domain position 1 (less accurate `landmask` position at the E peninsula) as boundary conditions. The second employed WRF outputs using domain position 2 (more accurate `landmask` position at the E peninsula) with modified settings (updated `SST` interpolation and `SST_SKIN` activation).

The impact of boundary condition changes in the VENTOS®/M simulations was most pronounced at T0978/E and T0960/N (Table 1). At the eastern peninsula (T0978/E), the modified WRF configurations contributed to lowering the simulated near-surface wind speed and the errors in DP2-MM-S, in comparison to DP1, reducing the RMSE by 6% (from 2.18 m s^{-1} to 2.05 m s^{-1}) and bias by 9% (from 1.35 m s^{-1} to 1.23 m s^{-1}). On the northern coastline (T0960/N), the DP2-MM-S microscale run showed a 12% increase in RMSE, despite a 17% reduction in bias, compared to the DP1 simulation. Meanwhile, at the other two tower locations (T0521/SE and T0522/S), the changes in boundary conditions had minimal impact on the microscale model results.

Overall, the explored WRF parameters exhibited a lower impact on the microscale runs compared to their influence on the mesoscale results. This occurred because, at the masts' location, only `HFX` and `TSK` are directly dictated by WRF results, and the WRF wind flow imposed on the lateral boundaries of the microscale domain lies outside the regions most affected by the WRF modifications. Additionally, while average values of mesoscale and microscale results showed relatively small differences due to parameter changes, at specific times of the day, wind speed differences reached up to 3 m s^{-1} in the model runs.

4. Conclusion

The simulations of the atmospheric flow over Madeira Island depicted the influence of the `landmask` positioning, `SST` interpolation, and `SST_SKIN` update on the near-surface wind at four tower locations (T0960/N at N, T0978/E at the E peninsula, T0521/SE at SE, and T0522/S at S).

By altering the mesoscale domain position to more accurately allocate the `landmask` (WRF-DP2), we obtained a better land/sea classification of Madeira's east peninsula. This led to a reduction of 19% in the RMSE and 67% in the bias of the WRF wind speed at the peninsula tower (T0978/E) compared to WRF-DP1 results.

Modifying the default `SST` interpolation in WRF's `METGRID.TBL` table, to account for missing and masked data (WRF-DP2-MM), improved the wind simulation at T0960/N (reducing RMSE and bias by 11% and 84%) and T0522/S (reducing RMSE and bias by 10% and 16%) in comparison to WRF-DP2 run. However, this change negatively affected the results at T0978/E, causing a 7% and 45% increase in RMSE and bias, attributed to an incorrect speedup in the WRF-DP2 simulation.

Using `SST_SKIN` in WRF (WRF-DP2-MM-S), which affects the temperature distribution at skin level, slightly improved the wind simulation only at T0521/SE (2% and 6% reduction in RMSE and bias) compared to WRF-DP2-MM results. This is attributed to the prevailing smaller-scale nature of the atmospheric circulation at T0521/SE, which differs from the circulation at T0960/N and T0978/E (primarily influenced by the trade winds) and at T0522/S (mainly affected by the Island's wake).

In the microscale simulations, where the boundary conditions were supplied by the WRF results, the changes had a less pronounced impact than in the mesoscale runs. Nonetheless, compared to VENTOS®/M DP1 at T0978/E, the simulated near-surface wind speed in VENTOS®/M DP2-MM-S reduced the RMSE and bias by 6% and 9%. Additionally, while average values of mesoscale and microscale results displayed relatively small differences due to parameter changes, certain times of the day showed wind speed differences up to $3\,\mathrm{m\,s^{-1}}$ in the model runs.

These results highlight the importance of considering different simulation parameters when modelling the wind in coastal and complex terrains, as well as emphasise the need for detailed analyses of simulation settings and outcomes, since small changes in configurations can have an impact on the simulation results, even further down the model chain.

Acknowledgments

This research was carried out within the scope of the LIdar Knowledge Europe (LIKE) project, H2020-MSCA-ITN-2019, funded by the European Union, Grant no. 858358. The meteorological data were provided by Observatório Meteorológico do Funchal/Instituto Português do Mar e da Atmosfera (IPMA), and the digital terrain model by Madalena Gonçalves and Duarte Klut (Direção Regional do Ordenamento do Território, DROTe).

Appendix

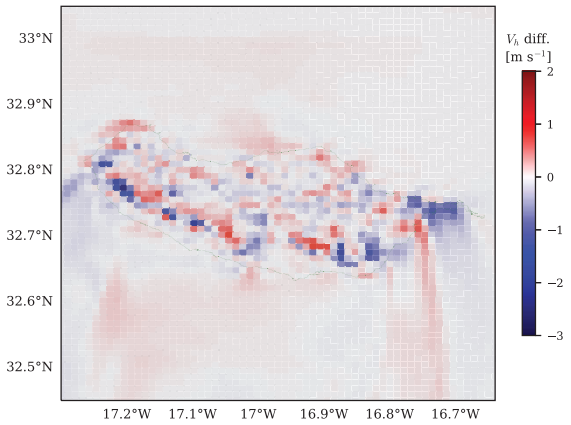

Figure A1. Difference between one-day average results (7 Aug 2016) of WRF DP2 and WRF DP1 (different `landmask` and domain position) horizontal wind speed at 10 m a.g.l. For the comparison, WRF DP1 results were interpolated onto the WRF DP2 grid.

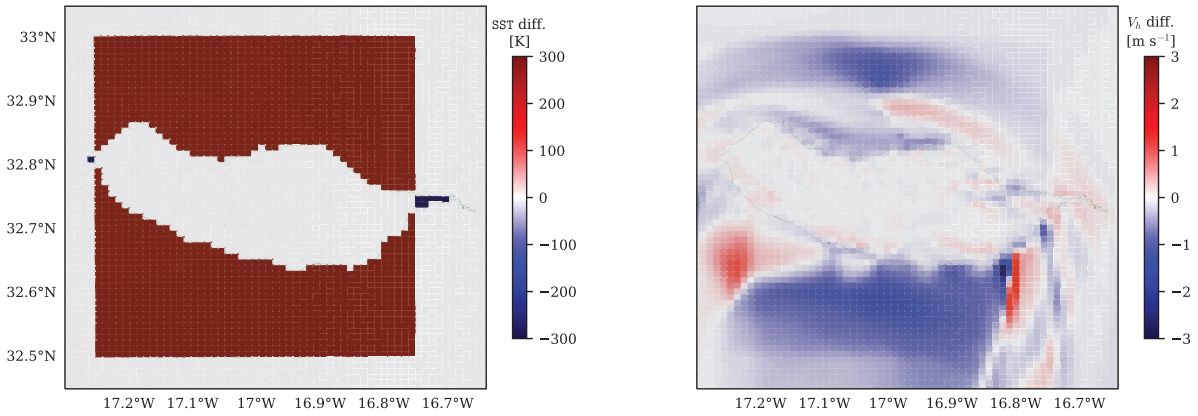

Figure A2. Difference between one-day average results (7 Aug 2016) of WRF DP2-MM and WRF DP2 (different `SST` interpolation method): `SST` (a) and horizontal wind speed at 10 m a.g.l. (b).

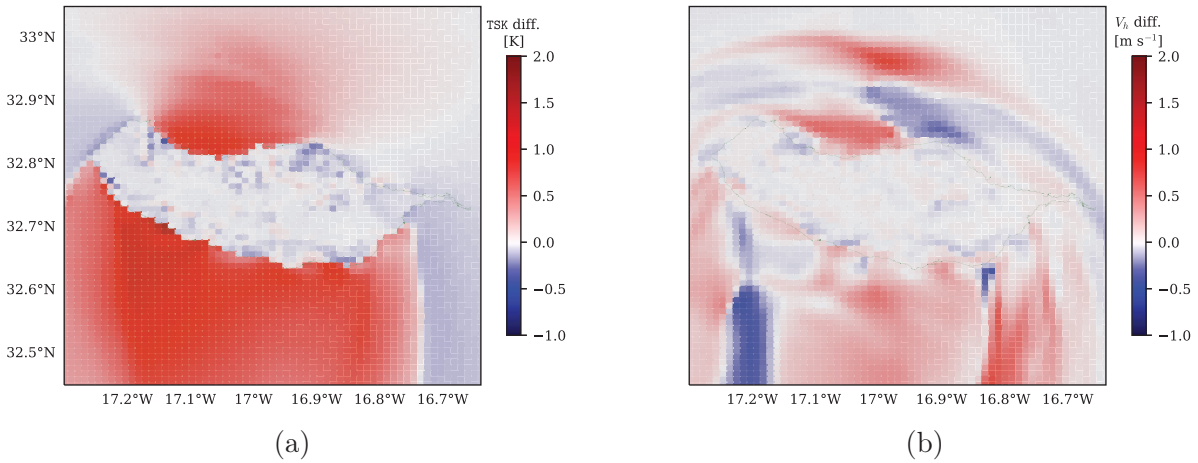

Figure A3. Difference between one-day average results (7 Aug 2016) of WRF DP2-MM-S and WRF DP2-MM (with and without `SST_SKIN`): `TSK` (a) and horizontal wind speed at 10 m a.g.l. (b).

References

[1] Grubišić V, Sachsperger J and Caldeira R M A 2015 *J. Atmos. Sci.* **72** 4755–4776
[2] Belo-Pereira M and Santos J A 2020 *Atmos.* **11** 1257
[3] Couvelard X, Caldeira R M A, Araújo I B and Tomé R 2012 *Dyn. Atmos. Oceans* **58** 128–149
[4] Miranda P M A, Tomé R, Frois L, Nogueira M, Alves J M R, Prior V, Caldeira R and Dutra E 2021 *Q. J. R. Meteorol. Soc.* **147** 679–690
[5] Skamarock W C *et al* 2019 A description of the advanced research WRF model version 4 Tech. rep. UCAR/NCAR
[6] Rodrigues C V, Palma J M L M and Rodrigues H 2016 *Bound.-Layer Meteorol.* **159** 407–437
[7] Farr T G *et al* 2007 *Rev. Geophys.* **45**
[8] Hersbach H *et al* 2020 *Q. J. R. Meteorol. Soc.* **146** 1999–2049

[9] Danielson J J and Gesch D B 2011 Global multi-resolution terrain elevation data 2010 (GMTED2010) Report 2011-1073
[10] Copernicus Land Monitoring Service 2018 CORINE land cover 2012
[11] Pineda N, Jorba O, Jorge J and Baldasano J M 2004 *Int. J. Remote Sens.* **25** 129–143
[12] Hahmann A N *et al* 2020 *Geosci. Model Dev.* **13** 5053–5078
[13] Hong S Y and Lim J 2006 *Asia-Pac. J. Atmos. Sci.* **42** 129–151
[14] Mlawer E J, Taubman S J, Brown P D, Iacono M J and Clough S A 1997 *J. Geophys. Res. Atmos.* **102** 16663–16682
[15] Dudhia J 1989 *J. Atmos. Sci.* **46** 3077–3107
[16] Jiménez P A, Dudhia J, González-Rouco J F, Navarro J, Montávez J P and García-Bustamante E 2012 *Mon. Weather Rev.* **140** 898–918
[17] Tewari M, Chen F, Wang W, Dudhia J, LeMone M A, Mitchell K, Ek M, Gayno G, Wegiel J and Cuenca R H 2004 Implementation and verification of the unified NOAH land surface model in the WRF model (Formerly paper number 17.5) *20th conference on weather analysis and forecasting/16th conference on numerical weather prediction* pp 11–15
[18] Hong S Y, Noh Y and Dudhia J 2006 *Mon. Weather Rev.* **134** 2318–2341
[19] Grell G A and Freitas S R 2014 *Atmos. Chem. Phys.* **14** 5233–5250
[20] Zeng X and Beljaars A 2005 *Geophys. Res. Lett.* **32** 2005GL023030
[21] Warner T T *Numerical Weather and Climate Prediction* (Cambridge University Press)